Geophysical Research Letters

RESEARCH LETTER
10.1029/2019GL086010

Observations Show That Wind Farms Substantially Modify the Atmospheric Boundary Layer Thermal Stratification Transition in the Early Evening

D. A. Rajewski[1], E. S. Takle[1], A. VanLoocke[1], and S. L. Purdy[1]

[1]Department of Agronomy, Iowa State University, Ames, IA, USA

Key Points:
- Wind turbines and wind farms generate turbulence at scales different from the natural atmosphere and modify the evening transition
- Wind turbine wakes shift the onset of near-surface stability ahead a few hours and shift the completion within the wake behind by 1 hr
- Differences in the transition are about 0.5 hr within an aggregate of wakes from multiple wind turbines in a large wind farm

Correspondence to:
D. A. Rajewski,
drajewsk@iastate.edu

Citation:
Rajewski, D. A., Takle, E. S., VanLoocke, A., & Purdy, S. L.. (2020). Observations show that wind farms substantially modify the atmospheric boundary layer thermal stratification transition in the early evening. *Geophysical Research Letters*, *47*, e2019GL086010. https://doi.org/10.1029/2019GL086010

Received 5 NOV 2019
Accepted 17 FEB 2020
Accepted article online 21 FEB 2020

Abstract Single wind turbines and large wind farms modify local scales of atmospheric boundary layer (ABL) turbulence through different mechanisms dependent on location within the wind farm. These changes in turbulence scales would most likely have notable influence on surface fluxes and microclimate during the afternoon and early evening stability transition. Profiles of Richardson number and shear and buoyancy from 1-Hz tall tower measurements in and near a wind farm in an agricultural landscape were used to quantify departures in stability characteristics during the fallow seasons. A single turbine wake decoupled turbulent connection between the surface and above the wind turbine, changed the onset of near-surface stabilization (earlier by a few hours), and lengthened the transition period (by up to an hour) within the rotor wake. Deep within a large wind farm, turbulence recovered to near-ambient conditions and departures of the transition onset and duration were within 30 min of the natural ABL.

Plain Language Summary Wind farms and single wind turbines change low-level atmospheric transport of momentum, heat, and water vapor, increase surface nighttime temperature, and decrease surface humidity. We infer that wind farms and single turbines also modify transitions in warming and cooling of the air during the daytime to nighttime hours. Measurements are used from a twin 120-m tall tower network in Iowa to detect differences in the evening transition between a location outside of a wind farm and near a single turbine or inside the wind farm. Behind a single turbine, the surface air cools 2 hr earlier while the air within the blade swept area cools 1 hr later when compared to outside the wind farm. Wind farm flow causes a small difference (±30 min) to the transition. The results provide additional evidence that wind turbines may influence biological regulation of soil microorganisms, plants, or animals in the proximity of wind energy production facilities.

1. Introduction

Expansion of renewable wind power generation for mitigating impacts from climate change (U.S. Department of Energy, 2015) has increased the global footprint of wind turbines and large wind farms in the marine and land atmospheric boundary layers (ABLs). Individual turbines and wind farms influence near-surface fluxes (Rajewski et al., 2014, 2016) and temperature, humidity, wind, and turbulence conditions below and above the rotor-swept layer (RSL; Adkins & Sescu, 2017; Armstrong et al., 2016; Platis et al., 2018; Siedersleben et al., 2018; Takle et al., 2019). Changes to the natural ABL diurnal transitions are expected because both wind farms and single turbines modify near-surface microclimate.

The natural ABL evening transition is responsible for changes in low-level convergence, mesoscale convection (Blackadar, 1957; Stensrud, 1996), and tornadic formation (Coffer & Parker, 2015). This transition influences wildlife (Alerstam, 2011), human aviation (Blackadar, 1957), wind power production (Deppe et al., 2012; Walton et al., 2014), and near-surface trapping of pests, pathogens, and pollutants (Takle et al., 1976). The early evening transition (EET) is the first few hours before and after sunset (Acevedo & Fitzjarrald, 2001; Bodine et al., 2009) during which the loss of buoyant heating at the surface leads to a rapid collapse of turbulence. The effect of the EET gradually extends into the residual mixed layer during evening and nighttime hours (e.g., Stull, 1988). EET turbulence is composed of local scales within the stable ABL and nonlocal scales from the residual layer that penetrate into the stable layer (Blay-Carreras et al., 2014; Sun et al., 2016). The growth of the stable surface layer during the EET causes a spike in low-level humidity (Acevedo & Fitzjarrald, 2001; Bonin et al., 2013), increases low-level stress divergence (Mahrt, 1981), and allows for the formation of a low-level jet (Klein et al., 2016).

During the EET, a crossover to neutrality occurs in the buoyancy flux and vertical potential temperature gradient (Jensen et al., 2016; Nadeau et al., 2011). The transition time for zero gradient or zero buoyancy may vary as much as a few hours due to natural variability in the ABL and surface-linked effects including latitude, terrain, vegetation, soil moisture, and temperature (e.g., Jensen et al., 2016). Forced scales of turbulence created by wind turbines may also influence ABL transitions.

Wind turbines generate turbulence with spectral energy on spatial scales of the rotor diameter and tip vortices (Jimenez et al., 2007; Vermeer et al., 2003). Over some daytime segments of the diurnal cycle, the energy contained at the turbine spectral scales is lower than ambient values, and microclimate influences are created by a decoupling of turbulence below turbine wakes from layers above (Rajewski et al., 2013; Takle et al., 2019). However, during the EET and into the nighttime, turbulent energy from wind turbines can dominate natural turbulence and be the key driver of microclimate processes. Wakes from single wind turbines and large wind farms reduce the rate of radiative surface cooling and enhance nighttime surface temperature (Baidya Roy & Traiteur, 2010; Harris et al., 2014; Zhou et al., 2012) and fluxes of heat, water, and carbon dioxide above crops (Rajewski et al., 2013, 2014). Such evening enhancement in surface heat flux was simulated across a 200-turbine wind farm (Lee & Lundquist, 2017). Changes in depth and intensity of wake wind speed, turbulent kinetic energy, and wind direction three rotor diameters downwind of a turbine were reported for one EET by Lee and Lundquist (2017) and Vollmer et al. (2017). However, other EET simulations indicate that turbine-generated turbulence is similar to neutral stratification conditions (Englberger & Dörnbrack, 2018; Sharma et al., 2017). Additional wind farm observations are necessary to improve predictive skill of wind energy-atmosphere interactions.

This study presents measurements of wind turbine and wind farm modification of EET characteristics for a flat terrain agricultural landscape within a U.S. Midwest low-density wind farm. Distinguishing impacts from an individual turbine and from impacts of the entire wind farm addresses differences in turbulence scales at the leading edge or deep within the wind farm. Single wake rotor-scale turbulence occupies a shallow ABL layer (e.g., 100 m) and should have a measureable impact on transition characteristics. The aggregation of turbulence scales from multiple wakes and the entrainment of natural turbulence into a thicker wind farm boundary layer (WFBL; e.g., >100 m) should reduce modification of the EET. Differences in stability casued by these forced scales of turbulence generation are compared to natural variations in background ABL turbulence.

2. Materials and Methods

One-Hertz in situ tower measurements of wind speed, air temperature, relative humidity, and air pressure from the Iowa Atmospheric Observatory (IAO) (Takle et al., 2019) are taken outside (A2) and inside (A1) a low-density 200-turbine Central Iowa wind farm with turbine spacing >15 rotor diameters, D (D = 82 m). Differences in onset, intensity, and duration characteristics of EET stratification are quantified within wakes 13–15 D downwind of a single wind turbine and from the wind farm wake (24–170 D from 50 turbines) as shown in figure 5 of Takle et al. (2019). Stability characteristics are determined from 5-min averages of 1-Hz measurements using the Gradient Richardson number, Ri, (e.g., Stull, 1988) as calculated in Takle et al. (2019). Gaps in sonic anemometer data prevent a climatological comparison of stability from direct measurement of turbulent fluxes. Ri and shear and buoyancy factors of Ri are calculated for the 5–40 m below rotor layer (BRL) beneath the turbine-swept rotor and the 40–120 m RSL of wind turbine blades (Newman et al., 2013; Takle et al., 2019). These stability terms are composited to determine contrasting conditions of the single turbine boundary layer (WTBL) and the WFBL from those of the natural ABL. Data from 6 June 2016 to 31 May 2018 are selected for analysis.

2.1. Filters for Data Quality and Nonideal Conditions

Spikes are removed from 5-min averaged measurements of wind speed and relative humidity at all tower heights and holds in wind speed and direction are filtered (Kelley & Ennis, 2016). March to May 2018 data are unusable because of a −9.0 K bias in air temperature and −0.9 hPa bias in air pressure caused by an electronic malfunction of the A1 instrument logger. Measurements are excluded when cloud cover is >2/8 oktas at either of two Automated Weather Observing System locations ~20 km east-northeast and west-northwest of A2. Precipitation and fog events from radar, satellite imagery, and surface visibility observations archived from the Iowa State University Iowa Environmental Mesonet Time Machine (2019) provide additional

filtering metrics. Seventeen percent of the total observations are then available to isolate surface conditions for the natural ABL, WTBL, and WFBL.

2.2. Selection of Surface Conditions and Sectors of Natural ABL, WTBL, and WFBL

Data are selected from seasonal periods with low surface roughness. Microclimate impacts from turbine wakes in these conditions are expected to be relatively large because of low wake dissipation when ambient shear-generated turbulence is small (Emeis, 2010). Measurements are composited for a soil/stubble surface and when the emerged crop has a low footprint on the soil surface: November (2016 and 2017) and March/April/May (2017 and 2018). Observations when snow cover was reported at either tower using modeled snow depth information from the National Operational Hydrologic Remote Sensing Center (2019) were removed. The A1 ABL sectors of no wind farm influence, WTBL, and WFBL are determined from the A2 80-m wind direction (Takle et al., 2019) and a 5° turbine wake expansion factor (Barthelmie et al., 2009). The natural ABL sector features a 5-m rise in terrain over a 100-m wide knoll 50 m west-southwest of the A1 tower. Measurements from this nonprevailing wind direction characterize terrain influences on the ABL distinguishing it from the other two directional sectors. To investigate afternoon shear convective ABL cases leading to an evening stable ABL, turbine-operating status conditions are selected when the 80-m wind speed at A2 is above the turbine cut-in speed (3.5 m s^{-1}) and below the wind speed of the turbine-specified rated power (11.5 m s^{-1}) (GE Energy, 2009). The temporal structure of the EET is analyzed from the remaining 3% of observations.

2.3. Determination of ABL Transition Periods

We define the natural ABL periods for EET according to departures from a reference sunset time (τ_s) (Mahrt, 2017). The measurements are composited for each standardized time into a 30-min period to reduce temporal variability leaving ~15–30 observations for each half-hour of the natural ABL, WTBL, and WFBL sectors.

2.4. Ri Profile Determination

Ri is calculated for the BRL and RSL (Takle et al., 2019). Sub-BRL/RSL levels of Ri are determined from gradients between adjacent measurement levels: 5–20 m, 20–40 m, 40–80 m, and 80–120 m. Each 5-min median Ri is composited to remove statistical outliers (Vanderwende et al., 2015; Vanderwende & Lundquist, 2016). Changes in BRL and RSL stability transition are identified by comparing A1 and A2 shear and buoyancy factors for each of the natural ABL, WTBL, and WFBL directional sectors. Sub-level Ri profiles are compared between A1 and A2 for the evolution of the EET at 30-min increments of standardized sunset times: 6, 5, 4, 3, 2, 1.5, 1, and 0.5 hr before sunset and 0, 0.5, 1.0, 1.5, and 2.0 hr after sunset.

3. Results

Differences in the EET are assessed by first describing transition conditions at the A2 tower surrounded by uniform soil surface and flat terrain (section 3.1). The EET onset and duration characteristics from A2 are compared with the A1 tower in each composite representing the knoll in the natural ABL, the WTBL, or WFBL flat terrain conditions in the BRL and RSL (section 3.2) and in higher vertical resolution of the 120-m layer (section 3.3).

3.1. EET Conditions in Flat Terrain ABL Outside the Wind Farm

Five-minute median composites of the A2 Ri shear term, Ri buoyancy term, and Ri for the BRL, RSL, and sublayers (Figure 1) indicate slight temporal and spatial variability of the onset and completion of the stability transition. The increase of wind shear from heating the mixed layer (Figure 1a) and a quasi-constant forcing of buoyancy (Figure 1b) during the afternoon ($t > \tau_s - 3.15$ hr) contribute to a gradual weakening of instability near the surface (Figure 1c). In the second phase of the afternoon transition ($\tau_s - 2.0$ hr $< t < \tau_s - 3.15$ hr) buoyancy begins to weaken with less insolation. In response, enhancement in shear further reduces instability below 40 m, continuing into the EET at onset ($t = \tau_s - 1.5$ hr) and completion ($t = \tau_s + 1.0$ hr). The Ri decrease above 40 m begins in the late afternoon ($t = \tau_s - 2.0$ hr) during the large decline in near-surface buoyancy associated with loss of frictional forces above the surface. The 5–20 m layer exhibits a 30-min earlier onset ($t = \tau_s - 1.5$ hr) of instability decay and 30-min earlier buoyancy transition to zero ($t = \tau_s - 0.5$ hr) than the 20–40 m layer. Destabilization at both sub-levels above 40 m is concurrent at the EET onset ($t = \tau_s - 1.5$

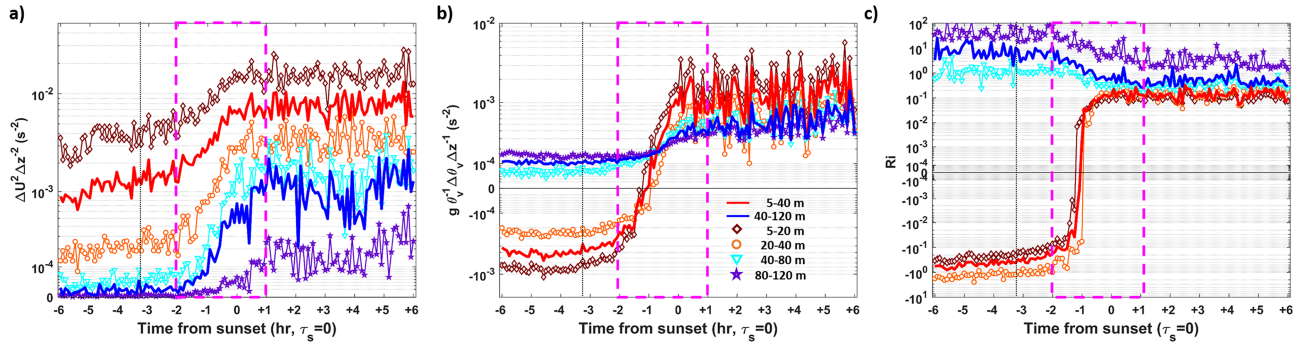

Figure 1. Five-minute median composites before, during, and after the EET in the 5–40 m BRL, 40–120 m RSL, and sublayers: 5–20 m, 20–40 m, 40–80 m, and 80–120 m for the (a) shear factor of Ri, (b) buoyancy factor of Ri, and (c) Ri for flat terrain ABL. The onset of slow decrease in instability preceding the EET is marked by a thin black line. A magenta dashed rectangle highlights the EET.

hr). Speed shear continues to rise during the EET throughout all sublayers, whereas buoyant suppression approaches a quasi-equilibrium intensity at sunset ($t = \tau_s$) in the 5–20 m layer to ~1 hr later in the 80–120 m layer. The concurrent leveling off in the stability decrease in the 40–80 m and 80–120 m layers indicates the completion of the EET below 120 m. Shear production is balanced by buoyant consumption for the remainder of the first few hours of the nighttime stable ABL (τ_s + 1.0 hr < t < τ_s + 6.0 hr).

3.2. Below-Turbine Layer and Turbine-Layer EET Characteristics From Natural and Forced Scales of Turbulence

We characterize EET variability in the BRL and the RSL shear and buoyancy factors between the tower sites due to the 5-m knoll (Figures 2a and 2d), a single turbine (Figures 2b and 2e), or the bulk of wind farm turbines at the A1 tower (Figures 2c and 2f). Overall, EET onset and duration characteristics at both towers and all ABL sectors are similar except during afternoon hours ($t = \tau_s - 4.5$ hr to $t = \tau_s - 0.5$ hr) in the WTBL BRL and the late stage of the EET ($t = \tau_s + 0.5$ hr to $t = \tau_s + 2.0$ hr) in both bulk layers in the WTBL and WFBL. Differences in shear and buoyancy between the towers are generally larger in the BRL than the RSL indicating the disruption of natural turbulence progression from the knoll, a single turbine wake, or multiple turbines in a large wind farm is most sensitive near the surface. The single turbine wake decouples turbulence above the rotor layer from the region below the rotor layer, which initiates smaller BRL instability in the middle afternoon and earlier stabilization (~1 hr) ahead of the natural flat ABL. However, in the WFBL, the conglomeration of multiple wakes reestablishes turbulent exchange above and below the RSL and follows the flat ABL changeover time to stable conditions (Figure 2f). After the EET ($t > \tau_s + 2.0$ hr), nighttime shear and stratification are more significantly reduced in the WTBL. These contrasts in EET characteristics between natural and forced scales of turbulence are amplified by determining higher-resolution Ri profiles in the next section.

3.3. Vertical Variations of the EET From Natural and Forced Scales of Turbulence

Afternoon and evening stability transitions are compared between the flat ABL to the knoll ABL, WTBL, and WFBL for additional sublayers of Ri (Figure 3). Each panel denotes (1) near-surface buoyancy decrease start times, (EET onset), (2) first level of the zero gradient crossover start times (ZGC start), (3) second level of zero gradient crossover end time (ZGC end), and (4) the time of positive slope of stability within all layers up to 120 m.

Temporal differences in the onset and ZGC transition in the flat ABL (Figures 3a, 3c, and 3e) are likely explained by fetch variations caused by gaps in adjacent field boundaries. Significant departures are observed from the flat ABL in the knoll ABL, WTBL, and WFBL. In the natural ABL, low variability of weakly stable stratification is noted above 40 m during the afternoon. However, a shift to unstable conditions occurs in the 80–120 m layer within the high shear deficit of the single turbine wake (Figure 3d), whereas reduced shear in the 40–80 m layer leads to an early afternoon strengthening of stability in the upper half of the WFBL (Figure 3f). Changes in the stability profile highlight the importance of entrainment of natural ABL fluxes and turbulence above the WFBL downward into the RSL. Both the single turbine wake and the

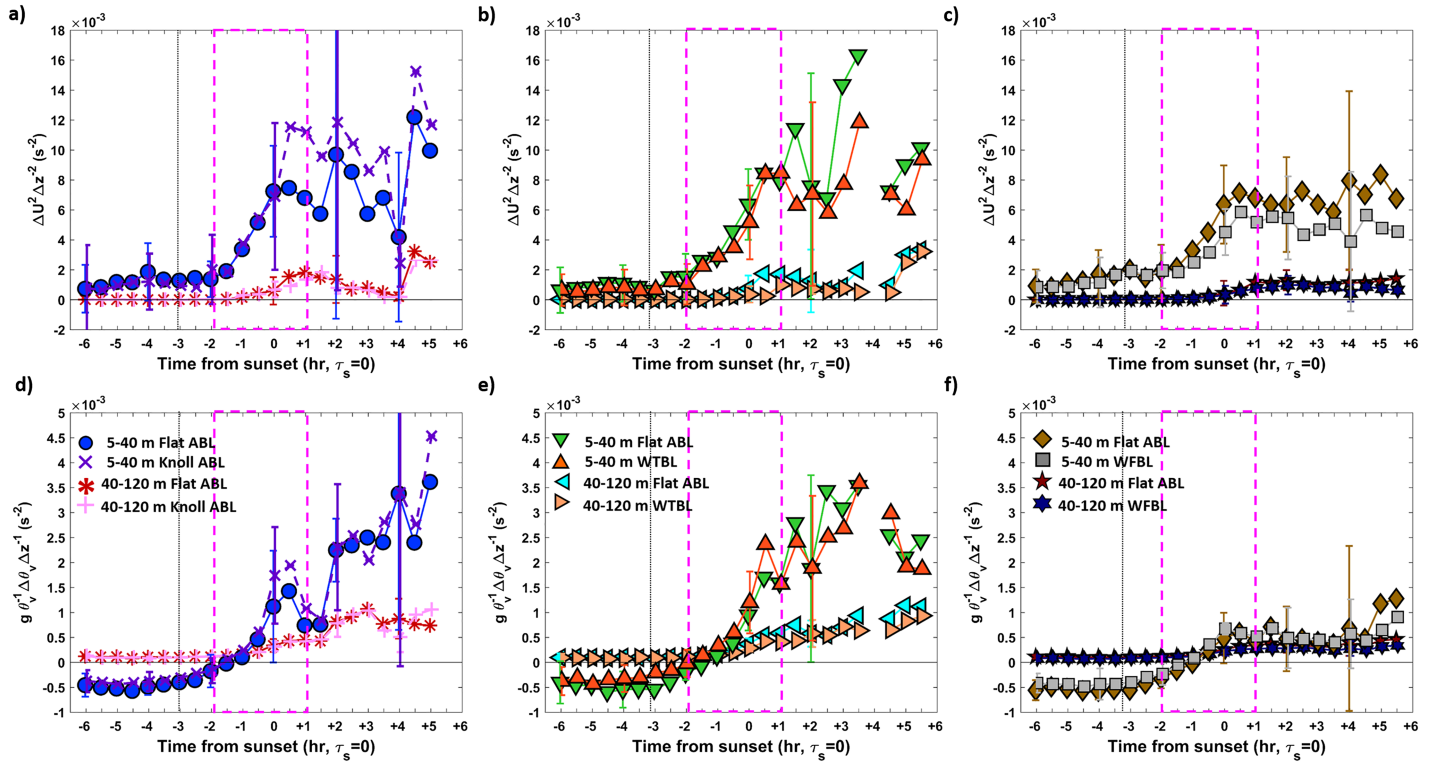

Figure 2. Thirty-minute median composite tower comparisons in the 5–40 m BRL and 40–120 m RSL of shear and buoyancy factors for flat ABL and knoll ABL (a, d), for flat ABL and WTBL (b, e), and flat ABL and WFBL (c, f). Error bars denote the interquartile range at selected 2-hr intervals during the afternoon and EET. The onset of slow decrease in instability preceding the EET is marked by a thin black line. A magenta dashed rectangle highlights the EET.

knoll shift the EET onset ahead by a few hours. The WTBL is behind 1 hr in the completion of the EET as indicated by the delayed stratification in the BRL/RSL interface. Evening progression of the stratification is only slightly modified by the WFBL.

4. Discussion

Rotor-scale turbulence induces the largest changes in afternoon and evening shear and buoyancy characteristics within and below a turbine wake in contrast to weaker differences deep in the wind farm. Findings are summarized (Figure 4) with a conceptual model of clear sky midday, afternoon, evening, and nighttime turbulence and flux characteristics of the ABL, WTBL, and WFBL. Our conception of the natural ABL (Figure 4a) is based on the canonical diurnal transition (Stull, 1988), observations from Bäserud et al. (2016) and Darbieu et al. (2015), and new understanding of counter-gradient transport by large coherent eddies (Sun et al., 2016). Color, size, and orientation of turbulent eddies denote changes in temporal-spatial turbulence structure, local/nonlocal scaling, intensity, and anisotropic quality. In the afternoon, the decoupling of large ABL eddies above the wind turbine rotor from the surface layer shortens the initiation time for stabilization by 1–2 hr in the lower half of the BRL (Figure 4b). In the evening, ambient turbulence above the RSL collapses due to the loss of buoyant heating; however, in the WTBL RSL, rotor-scale turbulence (e.g., 80 m) slows stabilization by up to 1 hr in the 20–40 m layer. Large coherent eddies, which disrupt the completion of near-surface stratification during the EET in the natural ABL, are unable to influence turbulence in the WTBL, thus further reinforcing BRL stabilization. For the WFBL, enhanced turbulence from the bulk of turbines in the wind farm weakly modifies shear and buoyancy indicating a recovery to ambient turbulence and transition characteristics within 30 min of the flat ABL (Figure 4c). Results indicate that relative forcing from single turbine wakes may be as significant as a step change in surface roughness or other heterogeneous forcing in modifying the EET (Calaf et al., 2014).

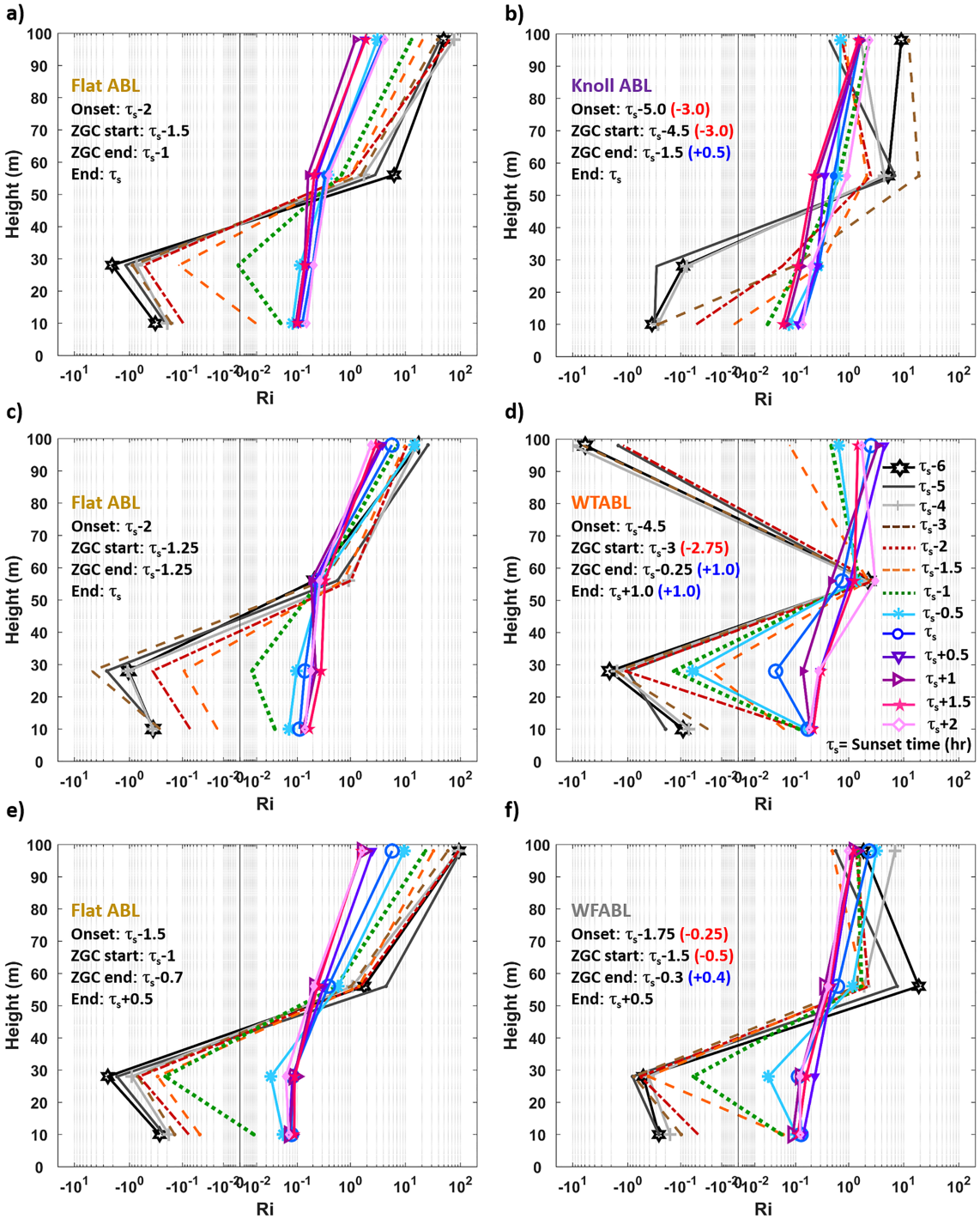

Figure 3. Thirty-minute median composites of the Ri profiles comparing the progression of the afternoon transition and EET stability of the flat ABL in (a), (c), and (e) to (b) knoll-influenced ABL, (d) WTBL, and (f) WFBL. Earlier/later departures from flat ABL in panels (a), (c), and (e) are denoted with red/blue text in panels (b), (d), and (f). Symbol sizes are scaled by number of samples for each category.

Large differences in the afternoon and EET characteristics between the knoll ABL and the flat ABL were unexpected. In addition to the slight slope in terrain west-southwest of A1, tillage management differences between A1 and A2 may influence tower measurements. Earlier near surface stabilization in the knoll may be related to flow perturbations from isolated low hills (Jackson & Hunt, 1975) and vegetative shelterbelts

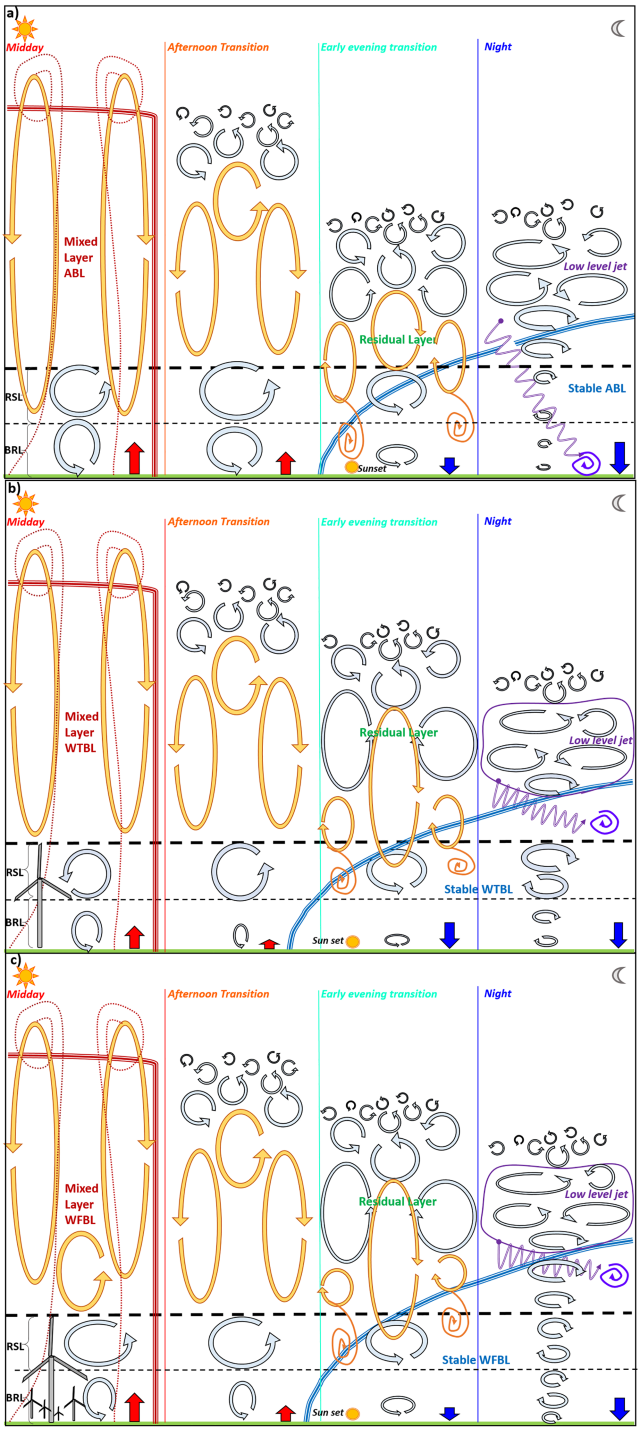

Figure 4. Conceptualization of (a) natural ABL transition, (b) forced WTBL transition, and (c) forced WFBL transition from midday unstable condition through the afternoon and EET until midnight stable stratification condition. Local eddies (gray), nonlocal coherent eddies (gold) during the daytime, and mesoscale sources of turbulence (purple) during the nighttime are shown.

(Wang et al., 2001). Accelerated wind speed, higher turbulence, and divergent flow in the barrier lee inhibits upward motion necessary for maintaining buoyancy (Tian & Parker, 2003). Therefore, natural variations in turbulence and microclimate from shelterbelts or terrain should be quantified to isolate turbulent forcing attributed from a single turbine or wind farm (Takle et al., 2019).

Limitations of interpreting stability from buoyancy and shear approximations to exact turbulent budget terms exist. The gradient method may be erroneous when vertical differences in wind speed and temperature are small or when ABL measurement resolution is >20 m (e.g., Balsley et al., 2008). Differences in buoyancy and shear are not concurrent during the EET, which potentially highlight the drawback of using a 30-min composite for the small data record available. Complete cases of the afternoon and EET are lacking due to temporal variability in wind direction and speed as wind moves between and outside of the knoll ABL, WTBL, and/or WFBL sectors. Sudden changes in wind speed intensity during and after the EET are represented as spikes and are filtered from the composites. Each sector is also conditioned by ambient stability. The largest impact of the EET was observed in the WTBL. More frequent (4%) unstable afternoon conditions were observed in the WFBL than the WTBL, whereas more frequent (2%) stable evening conditions were measured for the WTBL than for the WFBL. Knoll ABL cases were less than half as many as those from the dominant sector. Additional studies are warranted to isolate EET conditions in single wakes from those in wind farm wakes.

Detection of the natural ABL afternoon and evening transition within multiple layers below 120 m from the IAO demonstrates the need for high resolution, high fidelity temporal and spatial simulation of transition characteristics (Banta et al., 2013, 2018). This study indicates fast versus slow decay of wind shear between the BRL and RSL during the late afternoon and EET period. Simulations depict a few hours lag in the transition of buoyancy or temperature gradients between the surface and at higher levels in the ABL (Bosveld et al., 2014; Rodrigo et al., 2017), but these observations indicate a 30-min difference in transition phases.

Some of the measured contrasts of transition characteristics between the natural ABL and within single turbines and wind farms concur with simulations. Fitch et al. (2013) depict a 30-min earlier stabilization in the BRL and 30-min later completion of the stratification transition in the RSL as compared to the natural ABL. This earlier crossover of near-surface stability is indicated in IAO measurements of both single turbines and WFBLs unlike (Sharma et al., 2017). These EET and nighttime observations are in agreement on a substantial lowering of the shear factor (Fitch et al., 2013) and buoyancy factor (unlike Fitch et al., 2013; Sharma et al., 2017) within the WFBL. Limitations of these comparisons are due to different landscapes, climatic years, and synoptic-scale weather influences.

5. Conclusions

This study provides a first assessment of changes in the ABL afternoon and evening transitions within WTBLs and WFBLs from 120-m tall tower measurements outside and inside of a large wind farm. Highlights of notable findings are as follows:

1. Within the WTBL, the EET begins a few hours earlier and ends an hour later than in the flat ABL.
2. The WFBL modifies the transition start and completion by at most 30 min.
3. Heterogeneities in fetch and terrain regulate EET characteristics over an otherwise presumably flat uniform ABL.
4. Entrainment processes in the interaction of the ABL above and within the wind turbine/wind farm RSL need further assessment in understanding diurnal boundary layer transitions in wind farms.

These changes in the EET due to generation of turbulence from single wind turbines may influence transport of heat, water, and carbon dioxide from a non-vegetative surface. Turbine wakes are of equal or greater significance than ABL variability attributed from natural turbulence differences in surface and atmopheric factors. Equally important may be the modification of the morning transition characteristics from single turbine wakes or the wind farm wake, which is a topic of future study.

Acknowledgments
The authors acknowledge Daryl Herzmann for providing the data files used in the analysis. Financial support for tower construction was provided by the National Science Foundation Iowa EPSCoR Grant 1101284. Funding for data support, analysis, and interpretation is provided by the National Science Foundation Wind-Energy Science, Engineering and Policy IGERT Grant 1069283, National Science Foundation Grant 1701278, USDA Hatch Project IOW04414, and the Iowa Energy Center opportunity Grant OG-17-001. The authors acknowledge cooperation with the land owners and the wind farm manager. The authors declare no financial conflicts of interest. Data supporting this study are available at the Iowa State University open access research repository (https://www.doi.org/10.25380/iastate.11371506).

References

Acevedo, O. C., & Fitzjarrald, D. R. (2001). The early evening surface-layer transition: Temporal and spatial variability. *Journal of the Atmospheric Sciences*, *58*(17), 2650–2667. https://doi.org/10.1175/1520-0469(2001)058<2650:TEESLT>2.0.CO;2

Adkins, K. A., & Sescu, A. (2017). Observations of relative humidity in the near-wake of a wind turbine using an instrumented unmanned aerial system. *International Journal of Green Energy*, *14*(10), 845–860. https://doi.org/10.1080/15435075.2017.1334661

Alerstam, T. (2011). Optimal bird migration revisited. *Journal of Ornithology*, *152*, 5–23. https://doi.org/10.1007/s10336-011-0694-1

Armstrong, A., Burton, R. R., Lee, S. E., Mobbs, S., Ostle, N., Smith, V., et al. (2016). Ground-level climate at a peatland wind farm in Scotland is affected by wind turbine operation. *Environmental Research Letters*, *11*(4), 044024. https://doi.org/10.1088/1748-9326/11/4/044024

Baidya Roy, S., & Traiteur, J. J. (2010). Impacts of wind farms on surface air temperatures. *Proceedings of the National Academy of Sciences*, *107*(42), 17,899–17,904. https://doi.org/10.1073/pnas.1000493107

Balsley, B. B., Svensson, G., & Tjernström, M. (2008). On the scale-dependence of the Gradient Richardson number in the residual layer. *Boundary-Layer Meteorology*, *127*(1), 57–72. https://doi.org/10.1007/s10546-007-9251-0

Banta, R. M., Pichugina, Y. L., Brewer, W. A., James, E. P., Olson, J. B., Benjamin, S. G., et al. (2018). Evaluating and improving NWP forecast models for the future: How the needs of offshore wind energy can point the way. *Bulletin of the American Meteorological Society*, *99*(6), 1155–1176. https://doi.org/10.1175/BAMS-D-16-0310.1

Banta, R. M., Pichugina, Y. L., Kelley, N. D., Hardesty, R. M., & Brewer, W. A. (2013). Wind energy meteorology: Insight into wind properties in the turbine-rotor layer of the atmosphere from high-resolution Doppler lidar. *Bulletin of the American Meteorological Society*, *94*(6), 883–902. https://doi.org/10.1175/bams-d-11-00057.1

Barthelmie, R. J., Hansen, K., Frandsen, S. T., Rathmann, O., Schepers, J. G., Schlez, W., et al. (2009). Modelling and measuring flow and wind turbine wakes in large wind farms offshore. *Wind Energy*, *12*(5), 431–444. https://doi.org/10.1002/we.348

Bäserud, L., Reuder, J., Jonassen, M. O., Kral, S. T., Paskyabi, M. B., & Lothon, M. (2016). Proof of concept for turbulence measurements with the RPAS SUMO during the BLLAST campaign. *Atmospheric Measurement Techniques*, *9*(10), 4901–4913. https://doi.org/10.5194/amt-9-4901-2016

Blackadar, A. K. (1957). Boundary layer wind maxima and their significance for the growth of nocturnal inversions. *Bulletin of the American Meteorological Society*, *38*(5), 283–290. https://doi.org/10.1175/1520-0477-38.5.283

Blay-Carreras, E., Pardyjak, E. R., Pino, D., Alexander, D. C., Lohou, F., & Lothon, M. (2014). Countergradient heat flux observations during the evening transition period. *Atmospheric Chemistry and Physics*, *14*(17), 9077–9085. https://doi.org/10.5194/acp-14-9077-2014

Bodine, D., Klein, P. M., Arms, S. C., & Shapiro, A. (2009). Variability of surface air temperature over gently sloped terrain. *Journal of Applied Meteorology and Climatology*, *48*(6), 1117–1141. https://doi.org/10.1175/2009JAMC1933.1

Bonin, T., Chilson, P., Zielke, B., & Fedorovich, E. (2013). Observations of the early evening boundary-layer transition using a small unmanned aerial system. *Boundary-Layer Meteorology*, *146*(1), 119–132. https://doi.org/10.1007/s10546-012-9760-3

Bosveld, F. C., Baas, P., van Meijgaard, E., de Bruijn, E. I. F., Steeneveld, G. J., & Holtslag, A. A. M. (2014). The third GABLS intercomparison case for evaluation studies of boundary-layer models. Part A: Case selection and set-up. *Boundary-Layer Meteorology*, *152*(2), 133–156. https://doi.org/10.1007/s10546-014-9917-3

Calaf, M., Higgins, C., & Parlange, M. B. (2014). Large wind farms and the scalar flux over an heterogeneously rough land surface. *Boundary-Layer Meteorology*, *153*(3), 471–495. https://doi.org/10.1007/s10546-014-9959-6

Coffer, B. E., & Parker, M. D. (2015). Impacts of increasing low-level shear on supercells during the early evening transition. *Monthly Weather Review*, *143*(5), 1945–1969. https://doi.org/10.1175/mwr-d-14-00328.1

Darbieu, C., Lohou, F., Lothon, M., Vilà-Guerau De Arellano, J., Couvreux, F., Durand, P., et al. (2015). Turbulence vertical structure of the boundary layer during the afternoon transition. *Atmospheric Chemistry and Physics*, *15*(17), 10,071–10,086. https://doi.org/10.5194/acp-15-10071-2015

Deppe, A. J., Gallus, W. a., & Takle, E. S. (2012). A WRF ensemble for improved wind speed forecasts at turbine height. *Weather and Forecasting*, *28*(2), 212–228. https://doi.org/10.1175/WAF-D-11-00112.1

Emeis, S. (2010). A simple analytical wind park model considerating atmospheric stability. *Wind Energy*, *13*(5), 459–469. https://doi.org/10.1002/we.367

Englberger, A., & Dörnbrack, A. (2018). Impact of the diurnal cycle of the atmospheric boundary layer on wind-turbine wakes: A numerical modelling study. *Boundary-Layer Meteorology*, *166*(3), 423–448. https://doi.org/10.1007/s10546-017-0309-3

Fitch, A. C., Lundquist, J. K., & Olson, J. B. (2013). Mesoscale influences of wind farms throughout a diurnal cycle. *Monthly Weather Review*, *141*(7), 2173–2198. https://doi.org/10.1175/MWR-D-12-00185.1

GE Energy (2009). *1.5 MW wind turbine*. (GE Energy publication No. GEA14954C). [Brochure]. Retrieved from https://geosci.uchicago.edu/~moyer/GEOS24705/Readings/GEA14954C15-MW-Broch.pdf

Harris, R. A., Zhou, L., & Xia, G. (2014). Satellite observations of wind farm impacts on nocturnal land surface temperature in Iowa. *Remote Sensing*, *6*(12), 12,234–12,246. https://doi.org/10.3390/rs61212234

Iowa State University (2019). *Iowa Environmental Mesonet Time Machine*. Retrieved June 4, 2019, from https://www.mesonet.agron.iastate.edu/timemachine/

Jackson, P. S., & Hunt, J. C. R. (1975). Turbulent flow over a low hill. *Quarterly Journal of the Royal Meteorological Society*, *101*(430), 929–955.

Jensen, D. D., Nadeau, D. F., Hoch, S. W., & Pardyjak, E. R. (2016). Observations of near-surface heat-flux and temperature profiles through the early evening transition over contrasting surfaces. *Boundary-Layer Meteorology*, *159*(3), 567–587. https://doi.org/10.1007/s10546-015-0067-z

Jimenez, A., Crespo, A., Migoya, E., & Garcia, J. (2007). Advances in large-eddy simulation of a wind turbine wake. *Journal of Physics: Conference Series*, *75*, 012041. https://doi.org/10.1088/1742-6596/75/1/012041

Kelley, C. L., & Ennis, B. L. (2016). *SWiFT site atmospheric characterization*. (DOE publication No. SAND-2016-0216 618827). https://doi.org/10.2172/1237403

Klein, P. M., Hu, X. M., Shapiro, A., & Xue, M. (2016). Linkages between boundary-layer structure and the development of nocturnal low-level jets in Central Oklahoma. *Boundary-Layer Meteorology*, *158*(3), 383–408. https://doi.org/10.1007/s10546-015-0097-6

Lee, J. C. Y., & Lundquist, J. K. (2017). Observing and simulating wind-turbine wakes during the evening transition. *Boundary-Layer Meteorology*, *164*(3), 449–474. https://doi.org/10.1007/s10546-017-0257-y

Mahrt, L. (1981). The early evening boundary layer transition. *Quarterly Journal of the Royal Meteorological Society*, *107*(452), 329–343. https:/doi.org/10.1002/qj.49710745205

Mahrt, L. (2017). The near-surface evening transition. *Quarterly Journal of the Royal Meteorological Society*, *143*(708), 2940–2948. https://doi.org/10.1002/qj.3153

Nadeau, D. F., Pardyjak, E. R., Higgins, C. W., Fernando, H. J. S., & Parlange, M. B. (2011). A simple model for the afternoon and early evening decay of convective turbulence over different land surfaces. *Boundary-Layer Meteorology*, *141*(2), 301–324. https://doi.org/10.1007/s10546-011-9645-x

National Operational Hydrologic Remote Sensing Center (2019). *Interactive Snow Information*. Retrieved June 4, 2019, from https://www.nohrsc.noaa.gov/interactive/html/map.html

Newman, J., Lebron, J., Meneveau, C., & Castillo, L. (2013). Streamwise development of the wind turbine boundary layer over a model wind turbine array. *Physics of Fluids*, *25*(8), 085108. https://doi.org/10.1063/1.4818451

Platis, A., Siedersleben, S. K., Bange, J., Lampert, A., Bärfuss, K., Hankers, R., et al. (2018). First in situ evidence of wakes in the far field behind offshore wind farms. *Scientific Reports*, *8*(1), 2163. https://doi.org/10.1038/s41598-018-20389-y

Rajewski, D. A., Takle, E. S., Lundquist, J. K., Oncley, S., Prueger, J. H., Horst, T. W., et al. (2013). Crop wind energy experiment (CWEX): Observations of surface-layer, boundary layer, and mesoscale interactions with a wind farm. *Bulletin of the American Meteorological Society*, *94*(5), 655–672. https://doi.org/10.1175/BAMS-D-11-00240.1

Rajewski, D. A., Takle, E. S., Lundquist, J. K., Prueger, J. H., Pfeiffer, R. L., Hatfield, J. L., et al. (2014). Changes in fluxes of heat, H2O, and CO2 caused by a large wind farm. *Agricultural and Forest Meteorology*, *194*, 175–187. https://doi.org/10.1016/j.agrformet.2014.03.023

Rajewski, D. A., Takle, E. S., Prueger, J. H., & Doorenbos, R. K. (2016). Toward understanding the physical link between turbines and microclimate impacts from in situ measurements in a large wind farm. *Journal of Geophysical Research: Atmospheres*, *121*, 13,392–13,414. https://doi.org/10.1002/2016JD025297

Rodrigo, J. S., Allaerts, D., Avila, M., Barcons, J., Cavar, D., Chávez Arroyo, R. A., et al. (2017). Results of the GABLS3 diurnal-cycle benchmark for wind energy applications. *Journal of Physics: Conference Series*, *854*, 012037. https://doi.org/10.1088/1742-6596/854/1/012037

Sharma, V., Parlange, M. B., & Calaf, M. (2017). Perturbations to the spatial and temporal characteristics of the diurnally-varying atmospheric boundary layer due to an extensive wind farm. *Boundary-Layer Meteorology*, *162*(2), 255–282. https://doi.org/10.1007/s10546-016-0195-0

Siedersleben, S. K., Lundquist, J. K., Platis, A., Bange, J., Bärfuss, K., Lampert, A., et al. (2018). Micrometeorological impacts of offshore wind farms as seen in observations and simulations. *Environmental Research Letters*, *13*(12), 124012. https://doi.org/10.1088/1748-9326/aaea0b

Stensrud, D. J. (1996). Importance of low-level jets to climate: A review. *Journal of Climate*, *9*(8), 1698–1711. https://doi.org/10.1175/1520-0442(1996)009%3C1698:IOLLJT%3E2.0.CO;2

Stull, R. B. (1988). *An introduction to boundary layer meteorology*. Dordrecht: Kluwer Academic Publishers.

Sun, J., Lenschow, D. H., LeMone, M. A., & Mahrt, L. (2016). The role of large-coherent-eddy transport in the atmospheric surface layer based on CASES-99 observations. *Boundary-Layer Meteorology*, *160*(1), 83–111. https://doi.org/10.1007/s10546-016-0134-0

Takle, E. S., Rajewski, D. A., & Purdy, S. L. (2019). The Iowa Atmospheric Observatory: Revealing the unique boundary layer characteristics of a wind farm. *Earth Interactions*, *23*(2), 1–27. https://doi.org/10.1175/ei-d-17-0024.1

Takle, E. S., Shaw, R. H., & Vaughan, H. C. (1976). Low-level stability and pollutant-trapping potential for a rural area. *Journal of Applied Meteorology*, *15*(1), 36–42. https://doi.org/10.1175/1520-0450(1976)015<0036:LLSAPT>2.0.CO;2

Tian, W., & Parker, D. J. (2003). A modeling study and scaling analysis of orographic effects on boundary layer shallow convection. *Journal of the Atmospheric Sciences*, *60*(16), 1981–1991. https://doi.org/10.1175/1520-0469(2003)060<1981:amsasa>2.0.co;2

U.S. Department of Energy (DOE) (2015). *Wind vision: A new era for wind power in the United States* (DOE publication No. DOE/GO-102015-4557). Retrieved from https://www.energy.gov/sites/prod/files/WindVision_Report_final.pdf

Vanderwende, B., & Lundquist, J. K. (2016). Could crop height affect the wind resource at agriculturally productive wind farm sites? *Boundary-Layer Meteorology*, *158*(3), 409–428. https://doi.org/10.1007/s10546-015-0102-0

Vanderwende, B. J., Lundquist, J. K., Rhodes, M. E., Takle, E. S., & Irvin, S. L. (2015). Observing and simulating the summertime low-level jet in central Iowa. *Monthly Weather Review*, *143*(6), 2319–2336. https://doi.org/10.1175/MWR-D-14-00325.1

Vermeer, L. J., Sørensen, J. N., & Crespo, A. (2003). Wind turbine wake aerodynamics. *Progress in Aerospace Sciences*, *39*(6–7), 467–510. https://doi.org/10.1016/S0376-0421(03)00078-2

Vollmer, L., Lee, J. C. Y., Steinfeld, G., & Lundquist, J. K. (2017). A wind turbine wake in changing atmospheric conditions: LES and lidar measurements. *Journal of Physics: Conference Series*, *854*(1), 012050. https://doi.org/10.1088/1742-6596/854/1/012050

Walton, R. A., Takle, E. S., & Gallus, W. A. (2014). Characteristics of 50-200-m winds and temperatures derived from an Iowa tall-tower network. *Journal of Applied Meteorology and Climatology*, *53*(10), 2387–2393. https://doi.org/10.1175/JAMC-D-13-0340.1

Wang, H., Takle, E. S., & Shen, J. (2001). Shelterbelts and windbreaks: Mathematical modeling and computer simulations of turbulent flows. *Annual Review of Fluid Mechanics*, *33*(1), 549–586. https://doi.org/10.1146/annurev.fluid.33.1.549

Zhou, L., Tian, Y., Baidya Roy, S., Thorncroft, C., Bosart, L. F., & Hu, Y. (2012). Impacts of wind farms on land surface temperature. *Nature Climate Change*, *2*(7), 539–543. https://doi.org/10.1038/nclimate1505